NASA Technical Memorandum 102312
AIAA-89-2710

Performance of a 100 kW Class Applied Field MPD Thruster

Maris A. Mantenieks and James S. Sovey
National Aeronautics and Space Administration
Lewis Research Center
Cleveland, Ohio

Roger M. Myers
Sverdrup Technology, Inc.
NASA Lewis Research Center Group
Cleveland, Ohio

Thomas W. Haag and Paul Raitano
National Aeronautics and Space Administration
Lewis Research Center
Cleveland, Ohio

James E. Parkes
Sverdrup Technology, Inc.
NASA Lewis Research Center Group
Cleveland, Ohio

Prepared for the
25th Joint Propulsion Conference
cosponsored by the AIAA, ASME, SAE, and ASEE
Monterey, California, July 10-12, 1989

NASA

PERFORMANCE OF A 100 kW CLASS APPLIED FIELD MPD THRUSTER

M.A. Mantenieks, J.S. Sovey, T.W. Haag, and P. Raitano
National Aeronautics and Space Administration
Lewis Research Center
Cleveland, Ohio 44135

R.M. Myers and J.E. Parkes
Sverdrup Technology, Inc.
NASA Lewis Research Center Group
Cleveland, Ohio 44135

ABSTRACT

Performance of a 100 kW class, applied field MPD thruster was evaluated and sensitivities of discharge characteristics to arc current, mass flow rate, and applied magnetic field were investigated. Thermal efficiencies as high as 60%, thrust efficiencies up to 21%, and specific impulses of up to 1150 s were attained with argon propellant. Thrust levels up to 2.5 N were directly measured with an inverted pendulum thrust stand at discharge input powers up to 57 kW. It was observed that thrust increased monotonically with the product of arc current and magnet current.

NOMENCLATURE

J	arc current, A
J_m	magnet current, A
$\dot{m}$	mass flow rate, kg/sec
P_e	electric power, W (excludes magnet power)
$P_e/\dot{m}$	specific power, J/kg
P_l	power loss to the electrodes, W
P_o	inlet cold gas power, W
T	thrust, N
V	arc voltage, V
V_e	effective anode fall voltage, V
η	thrust efficiency, $T^2/2\dot{m}P_e$
η_{th}	thermal efficiency

INTRODUCTION

The magnetoplasmadynamic (MPD) thruster has potential propulsion applications for Earth-orbit transfer, maneuvering of large space systems, and interplanetary missions. The high thruster specific impulse (1000 to 5000 s) minimizes propellant requirements and the demands for mass transfer to low-Earth-orbit. MPD thruster missions in the next decades will probably employ solar or nuclear electric power systems in the 30 to 300 kW range. Farther term missions with interplanetary propulsion applications could use megawatt class nuclear power systems.

Recent interest in high power and interplanetary missions has reactivated the studies of steady-state MPD thruster technologies. Summaries of the early phases of MPD thruster work can be found in References 1-3. Most researchers have used pulsed or quasi-steady state MPD thrusters because of thruster/power system simplicity and modest vacuum facility requirements. Pulsed thrusters, operating for about 1 msec, are the only source of data concerning the discharge phenomena and performance limits of 1 to 10 MW class MPD arcjets. The most attractive specific impulse and thrust efficiency data to date have resulted from thrusters using hydrogen or lithium propellants. Since lithium propellant may not be desirable because of potential spacecraft and ground-based facility contamination issues, it is likely that steady-state thruster applications will involve the use of hydrogen or hydrogenic propellants. The power, thermal, and vacuum system requirements for megawatt class, steady-state thrusters operating with hydrogenic propellant exclude the use of most of the existing vacuum facilities in the United States. For example, a vacuum environment of less than 4×10^{-2} Pa (3×10^{-4} torr) is generally required to minimize the background gas entrainment effects on thruster performance (Ref. 4). Prior to 1972, a large percentage of the data for 10 to 100 kW inert gas, ammonia, or hydrogen thrusters were obtained at vacuum facility pressures in excess of 1.3 Pa (1.0×10^{-2} torr). It was shown that thrust uncertainties of 50 to 100 percent could exist because of gas entrainment in applied field devices (Refs. 3,4). More recently, self-field, steady state MPD thrusters using argon and nitrogen have been evaluated at vacuum tank pressures between 1 and 2.7 Pa (Ref. 5). These results showed that, for powers up to 75 kW, reliable self-field thruster data could be obtained at facility pressures less than 1.3 Pa.

This paper describes initial test results, including direct thrust measurements, in a MPD thruster test facility capable of providing reliable performance data for a steady-state, applied-field thruster operating up to 250 kW. A brief description of the test facility, including the vacuum chamber, power supplies, a closed cycle thruster water cooling system, and propellant metering is provided. Complete details of the test facility may be found in Reference 6.

Preliminary performance measurements are presented for a number of MPD thruster configurations operating at arc currents of up to 3000 A and arc powers of over 100 kW. For the convenience of the reader, some relevant data from Reference 6 are included in this report. Argon was mainly used as the propellant, but thermal efficiencies of helium, neon, and nitrogen are also reported. Basic thruster performance parameters discussed are discharge

characteristics, thrust measurements, thermal efficiencies, and magnetic field effects.

Diagnostic methods and instrumentation capable of measuring plasma parameters, current distribution, plasma species identification, and distribution of the cathode temperatures are described in Reference 7. The structure, operation, and performance characteristics of an inverted pendulum thrust stand are reported in Reference 8.

APPARATUS AND TEST PROCEDURE

The test facility consisted of the vacuum chamber, a MPD thruster and magnet, a propellant metering panel, water-cooling apparatus, the thrust stand, the power system, and a data acquisition system. This section provides descriptions of each of these systems.

MPD THRUSTER TEST FACILITY

The MPD thruster used in this investigation was a modified commercial coaxial plasma generator that is commonly used for plasma spraying (Ref. 9). This commercial device was selected because it was capable of routinely operating at 30 to 60 kW for extended periods of time and could be easily retrofitted with different anode and cathode designs. The various thruster configurations tested are shown in Fig. 1. All of the thrusters contained a copper anode assembly in which the water circuit was connected in series with the cathode water cooling hardware. The 13 mm diameter, 2 percent thoriated tungsten cathode was brazed to a water-cooled copper retainer. The anode and cathode were isolated using fluoropolymer and alumina insulators. Table I lists the relevant dimensions of the six thruster configurations that were evaluated. Thrust data were obtained with Thrusters D, E, and F.

In order to enhance the electromagnetic thrust component, the anodes were designed with larger channels (Refs. 10,11) and the current range was extended to 3000 A. The mass flow rates were also reduced to provide inlet pressures between 1.3 and 13 kPa (10 to 100 torr). Values of $J^2/\dot{m}$ ranged from $1x10^{10}$ to $3x10^{11}$ A^2-s/kg, which generally implied a significant electromagnetic thrust contribution (Refs. 3,12).

The magnet used in the present investigation (Fig. 2) was designed to provide a magnetic field of approximately 0.3 Tesla at the center of the magnet for a magnet current of 1500 A. It was a 14 cm I.D., 15 cm long solenoid consisting of 46 coils of copper tubing covered with glass sheath insulation. The magnet had four layers of ten coils each, and a final layer with six coils. Measured and calculated axial magnetic field strengths are shown in Fig. 3. The axial field strengths measured in the region of the cathode tip and the thruster exit plane were about 0.23 and 0.16 T, respectively, for a magnet current of 1400 A.

The thrust stand, fully described in Reference 8,and shown in Fig. 4, was an inverted pendulum whose upright flexures were designed to deflect about 5 cm at a thrust of 5 N. The pivoting structure of the thrust stand transferred the weight of the thruster to a system of flexures anchored to the lower

frame. The flexures pivoted about an axis 1.5 m below the thruster centerline. The major restoring force was provided by the 16 mm diameter primary flexures. The time derivative of the thrust stand displacement was used to drive an electromagnetic damper. Thrust stand displacement was measured by a movable iron core in a linearly variable differential transformer (LVDT) which was mounted to a fixed reference structure. The thrust stand assembly contained a remotely controlled leveling mechanism to vary the angle of the stand and adjust the LVDT signal. Remote calibration of the stand was obtained by applying small weights along the thrust axis using monofilament line and a precision pulley.

Tares due to thruster discharge current were shown to be negligible. Tares due to the applied magnetic field were reduced, after considerable effort, to values less than 3.0 percent of measured thrust for arc discharge currents between 1000 to 2500 A and magnet currents up to 1000 A. The tares due to the applied field could be determined independently and were subtracted from the indicated thrust measurement. Thermally induced drift of the thrust signal was on the order of 50 mN during test runs of about an hour and this drift could also be accounted for by an in-situ thrust calibration procedure.

The thruster and thrust stand were mounted to a vacuum chamber bulkhead and were inserted into a 3 m diameter by 3 m long port. The vacuum chamber was evacuated using nineteen, 0.8 m diameter hydrocarbon oil diffusion pumps with freon traps cooled to 236 K. Maximum allowable flow rates for helium, nitrogen, and argon were about $4.5x15^{-6}$, $8.0x15^{-6}$, and $15x10^{-6}$ kg/s, resepctively, for a main chamber pressure of $7x10^{-2}$ Pa ($5x10^{-4}$ torr).

The propellant feed system was designed to provide three parallel gas paths such that one or more gases might be available for thruster operation. Flowmeter ranges were 0.5, 5, and 50 standard liters of nitrogen per minute. Flowmeter accuracy was estimated to be within 2 percent over the range of 10 to 100 percent of full-scale. The flowmeters were directly calibrated with argon and helium. Measured values of nitrogen and neon flow rates were based on the vendor's calibration factors.

The thruster inlet pressure was sensed using a capacitance manometer. While the thruster chamber pressure could not be measured directly, the inlet pressure provided an upper bound of the chamber pressure, as a significant pressure drop probably existed across the propellant injector.

Water cooling to the arc and magnet was provided by two separate pump/heat exchanger assemblies capable of supplying 0.8 liter/s of water at a pressure of 1 MPa. The MPD thruster cathode and anode were cooled by the same pump/heat exchanger using de-ionized, distilled water in the closed-loop system. Water flow rate data were obtained from a calibrated turbine meter. The power lost to the electrodes was obtained by measuring the water flow rate and the change in water temperature. Digital readouts were used to indicate the water temperature to the nearest degree Fahrenheit.

The power system was composed of the arc supply, a high voltage arc starter, the magnet supply, and safety sensors and interlocks. The arc supply consisted of four welding power supplies connected in a series-parallel

arrangement which were isolated from the vacuum facility ground to minimize extraneous arcing. Maximum output power capability was 264 kW at 3000 A and 88 V. The open circuit voltage was 160 V. Arc voltage was directly measured with potential leads across the MPD thruster. The arc was started using a 950 V, half-wave rectifier connected to the thruster via a 100 ohm resistor. A single welding supply provided power to the electromagnet. Maximum steady state current was 1500 A. The power supply was isolated from ground as well as from the arc supply.

PROCEDURE

The arc was started by setting the argon flow rate to approximately 5.0×10^{-4} kg/sec, initiating a low current, glow discharge from the starter supply, and activating the arc supply which was preset for 2000 A operation. Approximately four seconds after arc ignition, the arc current was reset to 1000 A and the arc starter was turned off. The flow rate was then reduced to about 9.0×10^{-5} kg/sec which was more typical of the low pressure MPD arc operation. In all cases, the arc was started with argon propellant. Transition to another propellant was accomplished by closing the argon isolation valve and opening the valve for the desired propellant.

The major thruster variables were mass flow rate, arc current, and magnet current. The propellant flow rate was chosen to be high enough to provide stable discharge operation but low enough to yield values of $J^2/\dot{m}$ in the 1×10^9 to 1×10^{11} A^2-s/kg, which are representative values for low pressure MPD thrusters (Ref. 3). The upper limit of the arc current was selected to prevent thermal failure of the water coolant O-rings in the anode assembly. The range of magnet currents was defined by a minimum current ($\sim$500 A) to provide a stable discharge and by the magnet power supply limit 1500 A.

During thruster operation, the anode potential was found to float within 10 V of facility ground at argon flow rates in excess of 4.0×10^{-5} kg/sec. However, the anode floated to about 40 V above ground at very low flow rates of 8.0×10^{-6} kg/sec. In all cases, there was very little evidence of arcing external to the thruster as long as the arc supply was floating, the power cables were insulated, and the facility pressure was less than 7×10^{-2} Pa.

Thrust measurements were obtained after approximately 20 minutes of thruster operation at constant operating conditions. The thruster was then turned off to obtain a zero thrust reference level and to measure tares due to the applied magnetic field.

RESULTS AND DISCUSSION

Preliminary experiments, with several MPD thruster configurations (Fig. 1), were directed at determining the sensitivity of discharge parameters to geometry and propellant flow rate (Ref. 6). The following discussion will focus on experiments to gain insight into MPD thruster performance by examining: 1) thermal efficiency, 2) effective anode voltage drops, and 3), thrust measurements over a range of thruster configurations, operating conditions, and applied magnetic fields.

THERMAL EFFICIENCY

It has been observed that a large fraction of the MPD thruster input power was deposited in the electrodes at input power levels up to about 300 kW. For example, in previous work the maximum power available for thrust production with hydrogen, ammonia, and argon MPD arcjets was typically 80, 70, and 60 percent of the input power, respectively (Refs. 5, 13, and 14). These data were obtained from water-cooled devices which are less efficient and are presumed to have larger anode voltage drops than radiation-cooled MPD thrusters (Ref. 2). The thermal efficiency is defined as:

$$\eta_{th} = \frac{P_e + P_o - P_l}{P_e + P_o} \doteq 1 - P_l/P_e \qquad (1)$$

The cold gas power, P_o, was neglected in the calculations since it was less than 0.3 percent of the electric power for all data reported. To simplify comparison of data, the magnet power was not included in the parameter, P_e.

An effective anode fall voltage may be defined as:

$$V_e = P_l/J \qquad (2)$$

and has been used by others in describing anode loss phenomena (Ref. 15). In Fig. 5, the effective anode fall voltage is plotted against specific power for argon, neon, and helium propellants. In this figure, the data from thruster configurations E and F have been added to data found in Reference 6. Thrusters, operating at specific powers of 37 to 100 MJ/kg, had effective anode fall voltages between 10 to 15 V. Thrusters operating in this range had inlet pressures in excess of 13 kPa and values of $J^2/\dot{m}$ between 1.8 and 7.1 $\times 10^9$ A^2-s/kg. The MPD thrusters operating at higher specific powers and higher values of $J^2/\dot{m}$ had effective anode fall voltages between 15 to 30 V which were a major fraction of the arc voltages measured using Thrusters A to F.

The $\dot{m}^{1/2}V$ parameter was used in Reference 6 to correlate the thermal efficiency data for argon, helium, nitrogen, and neon using Thrusters A-D. The data for thruster configurations E and F were added to the data of Reference 6 and are shown in Fig. 6. The data were taken between 1 and 3 kA. The thermal efficiency was shown to be very sensitive to the $\dot{m}^{1/2}V$ parameter in the 0.13 to 0.32 V-$kg^{1/2}s^{-1/2}$ range. The data where the thermal efficiency appears to approach an asymptote are thermal arc results (high mass flow rates and dominant Joule heating). The conical anode thrusters (E and F) exhibited higher anode losses and these data did not follow the thermal efficiency trends of the straight channel thrusters (A-D). A clear parametric relationship between the thermal efficiency data and arc current, $J^2/\dot{m}$, power, or specific power was not evident.

THRUST MEASUREMENTS

Thrust measurements, as a function of arc power, are shown in Fig. 7. Thruster configurations D,E, and F were evaluated with argon propellant. The power was increased at a given arc current by increasing the applied magnetic

field which produced an increase in arc voltage. The measured thrust increased nearly linearly with power at constant arc current. Thrust levels between 0.8 and 2.5 N were obtained over a 20 to 62 kW range of input electric power.

Fig. 8 shows the specific impulse as a function of specific power for the various thruster configurations using argon. The specific impulse also increased almost linearly with increasing specific power at constant arc current. The highest values of specific impulse ($\sim$1100 s) were obtained with thruster configurations E and D at discharge currents of 1000 and 1500 A, respectively.

The data of a thermal arcjet and a self-field MPD thruster from References 16 and 17, respectively, are included in Fig. 8 for comparison. The specific impulse of 720 s, attained with an argon thermal arcjet is the highest value of specific impulse found in the available literature for that operating mode. The specific impulse levels of Thrusters D and E exceeded the thermal arcjet data by more than 50% implying electromagnetic field thrust augmentation was significant.

Arc currents of 1000 to 1500 A ($J^2/\dot{m}$ of 6.3×10^9 and 1.4×10^{10} A^2-s/kg) were required to attain 1100 s specific impulse using Thrusters E and D, respectively, with argon propellant. These results compare favorably to the self-field MPD thruster which provided a specific impulse of 1200 s at a J^2/m of 2.8×10^{10} A^2-s/kg. In all three cases, the overall thrust efficiency was between 0.21 and 0.24.

Figure 9 depicts the thrust to power ratio as a function of specific impulse for the various thrust configurations. As mentioned previously, most of the thrusters did not operate stably below a magnet current of 500 A; however, on several occasions Thruster D was stable long enough to permit a thrust measurement. As the data from Thruster D at an arc current of 1000 A indicate, there was a steep increase in the ratio of thrust to power as the magnetic field current was increased from zero to approximately 500 A. The increase in the thrust to power ratio was 50% with an associated 64% increase in the specific impulse over the applied magnetic field increment. Further increases in magnetic field resulted in increases of specific impulse without a noticeable thrust to power ratio decrease. This trend was observed for both thruster configurations (D and F).

The thermal and thrust efficiencies of the thruster configurations D,E, and F are shown in Fig. 10. Thermal efficiencies as high as 0.47 were obtained with the flared anode thruster using argon propellant. Generally, lower thermal efficiencies were observed as arc current was increased from 1000 to 1500 A. This change usually resulted in lower arc voltage and a higher effective anode voltage drop as shown in Figure 5. Both thrusters D and E, operating at 1000 A, converted 39 to 47 percent of available power ($P_e - P_l$) for propulsion to thrust power. This is a rather high fraction since approximately 15 to 20 percent of the power available for propulsion must be consumed to fully ionize the argon.

The highest thrust efficiencies (21%) were obtained with thruster configurations D and E. Because of arc instabilities and thermal problems, thruster configuration F was constrained to operate at higher propellant mass flow rates, thus limiting the maximum attainable specific impulse to 700 s. Thrust efficiencies of 20 to 25% with argon have been reported with water-cooled, self-field, and pulsed thrusters (Refs. 10,13). The thrust efficiencies of the three thruster configurations (D,E, and F) operating at the various arc currents tended to increase as the specific impulse was increased by an increasing magnetic field.

It should be mentioned that discharge characteristics were not always repeatable from day to day while operating at the same thruster parameters. A possible reason for this may be that the cathodes, while being of the same geometry, may not have had similar emission characteristics due to thoria depletion or due to cooling water leaks because of failure of water seals. Current distribution measurements also indicated different profiles for similar thruster configurations and identical operating parameters (Ref. 7), indicating that the observed voltage differences are not totally attributable to electrode fall voltages. Cathode deterioration was also evidenced by difficulty in establishing an arc discharge. More detailed studies of MPD thruster discharge characteristics and the plasma exhaust are required to understand this behavior.

MAGNETIC FIELD EFFECTS

The application of a magnetic field to the MPD thruster had two primary effects: first, it enlarged the operating envelope of the thruster in which stable operation was achieved; second, the performance increased with increasing magnetic field. The first result has been observed by previous investigators (Refs. 12,14,15). The second result also was to be expected, because the applied field introduces additional force terms besides the electrothermal term, and the "pumping" and "blowing" force terms due to self-induced fields (Ref. 2). Due to the complications arising from the interactions of these forces, no universally accepted model for applied field MPD thruster operation exists.

Following the practice of previous investigators, the thrust in Fig. 11 was plotted as a function of the product of the arc current and magnet current for thruster configurations D, E, and F. All of the thrusters exhibit a monotonic dependence with arc current-magnet current product. This result is similar to previous investigations (Refs. 17-21).

For thruster configuration D, the thrust increased by 64% as the applied magnet current increased from 0 to 1500 A. These results indicate that the thrust should increase monotonically with product of the arc current and magnet currents up to 2.2×10^6 A^2. In contrast to References 22 and 23, no saturation effect with increasing magnet current was found.

CONCLUDING REMARKS

Performance of 100 kW class, applied field MPD thrusters were evaluated. Six thruster configurations were characterized as functions of discharge current, mass flow rate, and applied magnetic field. Thrust measurements were obtained with three of the thruster configurations.

Higher arc voltages and thermal efficiencies were obtained using the larger diameter anode channel (26 mm) thruster with a flared anode. Representative effective anode fall voltages, estimated by anode power losses ranged from 15 to 30 V. Thermal efficiencies as high as 60 percent were obtained using argon as the propellant; however, measured thrust efficiencies were limited to only 21%. A thrust of 2.5 N was measured at an arc discharge power of 57 kW. The highest measured specific impulse was 1150. This specific impulse compares favorably with values found in the literature using self-field MPD thursters at comparable $J^2/\dot{m}$ parameters. The thrust to power ratio was nearly constant with increasing specific impulse at magnetic current values of greater than 500 A. Finally the measured thrust was shown to be monotonically inceasing with the product of the arc and magnet currents.

REFERENCES

1. Nerheim, N.M. and Kelly, A.J., "A Critical Review of the State-of-the-Art of the MPD Thruster," AIAA Paper 67-688, Sept. 1967.

2. Seikel, G.R., York, T.M., and Condit, W.C., "Applied-Field Magnetoplasmadynamic Thrusters for Orbit-Raising Missions," Orbit-Raising and Maneuvering Propulsion: Research Status and Needs. (Progress in Astronautics and Aeronautics, Vol. 89), L.H. Caveny, Ed., AIAA, New York, 1984, pp. 260-286.

3. Sovey, J.S. and Mantenieks, M.A., "Performance and Lifetime Assessment of MPD Arc Thruster Technology," AIAA Paper 88-3211, July 1988 (NASA TM-101293).

4. Sovie, R.J. and Connolly, D.J., "Effect of Background Pressure on Magnetoplasmadynamic Thruster Operation," Journal of Spacecraft and Rockets, Vol. 7, No. 3, Mar. 1970, pp. 255-258.

5. Kurtz, H.L., Auweter-Kurtz, M., and Schrade, H.O., "Self-Field MPD Thruster Design - Experimental and Theoretical Investigations," AIAA Paper 85-2002, Sept. 1985.

6. Sovey, J.S., Mantenieks, M.A., Haas, T.W., Raitano, P., and Parkes, J.E., "Test Facility and Preliminary Performance of a 100 kW Class MPD Thruster," NASA TM-102021, 1989.

7. Myers, R., "Plume Characteristics of MPD Thrusters: A Preliminary Examination," AIAA Paper 89-2832, July 1989.

8. Haag, T.W., "Design of Thrust Stand for High Power Electric Propulsion Devices," AIAA Paper 89-2829, July 1989.

9. Product Data Sheet 387-1, Electro-Plasma, Inc., Irvine, CA, 1988.

10. Jahn, R.G., Physics of Electric Propulsion, McGraw-Hill Inc., New York, 1968.

11. Wolff, M., Kelly, A.J., and Jahn, R.G., "A High Performance Magnetoplasmadynamic Thruster," 17th International Electric Propulsion Conference, Japan Society for Aeronautical and Space Sciences, Tokyo, Japan, 1984, pp. 206-212.

12. Malliaris, A.C., John, R.R., Garrison, R.L., and Libby, D.R., "Quasi-Steady MPD Propulsion at High Power," AVSD-0146-71-RR, Avco Corp., Wilmington, MA, Feb. 1971, NASA CR-111872.

13. Ducati, A.C., Muehlberger, E., and Todd, J.P., "Design and Development of a Thermo-Ionic Electric Thruster," NASA CR-59804, 1964.

14. Bennett, S., Enos, G., John, R., and Powers, W., "Magnetoplasmadynamic Thrustor Research," AVSSD-272-67-RR, AVCO Corp., Space Systems Div., Lowell, MA, May 1967, NASA CR-72345.

15. Cann, G.L., Harder, R.L., Moore, R.A., and Lenn, P.D., "Hall Current Accelerator," ESOC-5470-Final, Electro-Optical Systems Inc., Pasadena, CA, 1966, NASA CR-54705.

16. Kurtz, M.L., Auweter-Kurtz, M., Glocker, B., Merke, W., and Schrade, H.O., "A 15-kW Experimental Arcjet," IEPC Paper 88-107, Oct. 1988.

17. Merke, W.D., Auweter-Kurtz, M., Habiger, H., Kurtz, H., and Schrade, H.O., "Nozzle Type MPD Thruster Experimental Investigations," IEPC Paper 88-028, Oct. 1988.

18. Patrick, R.M. and Schneiderman, A.M., "Performance Characteristics of a Magnetic Annular Arc," AIAA Journal, Vol. 4, No. 2, Feb. 1966, pp. 283-290.

19. Kagaya, Y., Yoshikawa, T., and Tahara, H., "Quasi-Steady MPD Arcjets with Applied Magnetic Fields," AIAA Paper 85-2001, Oct. 1985.

20. Fradkin, D.B., Blackstock, A.W., Roehling, D.J., Stratton, T.F., Williams, M., and Liewer, K.W., "Experiments Using a 25-kW Hollow Cathode Lithium Vapor MPD Arcjet," AIAA Journal, Vol. 8, No. 5, May 1970, pp. 886-894.

21. Fradkin, D.B., "Analyses of Acceleration Mechanisms and Performance of an Applied Field MPD Arcjet," Ph.D. Thesis, Princeton University, 1973.

22. Kimura, I. and Arakawa, Y., "Effect of Applied Magnetic Fields on Physical Processes in an MPD Arcjet," AIAA Journal, Vol. 15, No. 5, May 1977, pp. 721-724.

23. Connolly, D.J., Bishop, A.R., and Seikel, G.R., "Tests of Permanent Magnet and Superconducting Magnet MPD Thrusters," AIAA Paper 71-696, June 1971, (NASA TM X-67827).

TABLE I - THRUSTER CONFIGURATIONS

THRUSTER DESIGNATIONS	ANODE CHANNEL DIAMETER mm	CHANNEL LENGTH,[a] cm	ANODE FLARE HALF ANGLE/LENGTH, deg /cm
A	16.5	5.3[b]	0/0
B	16.5	4.1[b]	0/0
C	26	4.2[b]	0/0
D	26	4.2[b]	41°/1.1
E	26[d]	5.4[b]	10.5°/5.4
F	26[d]	5.4[c]	10.5°/5.4

a Upstream end of cathode to anode exit plane
b Cathode diameter 1.27 cm, cathode length 2.2 cm
c Cathode diameter 1.27 cm, cathode length 3.8 cm
d Inlet diameter

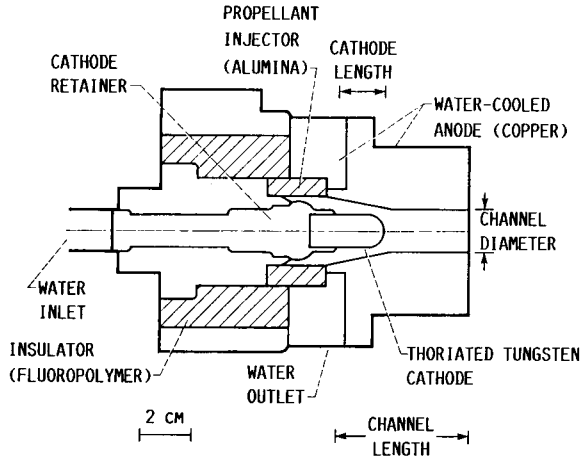

(A) MPD THRUSTER (A OR B) WITH CYLINDRICAL ANODE. (REF. 6).

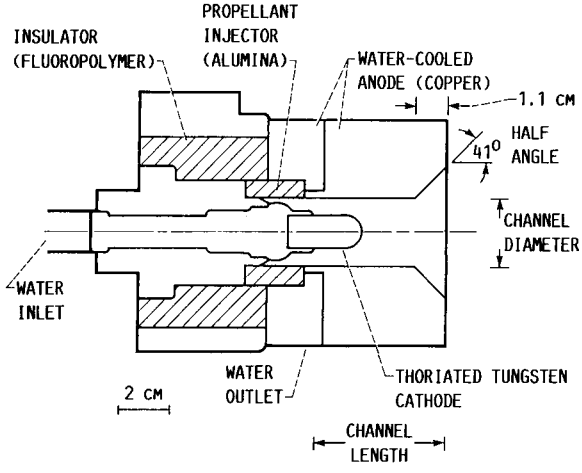

(B) MPD THRUSTER (D) WITH FLARED ANODE. (REF. 6).

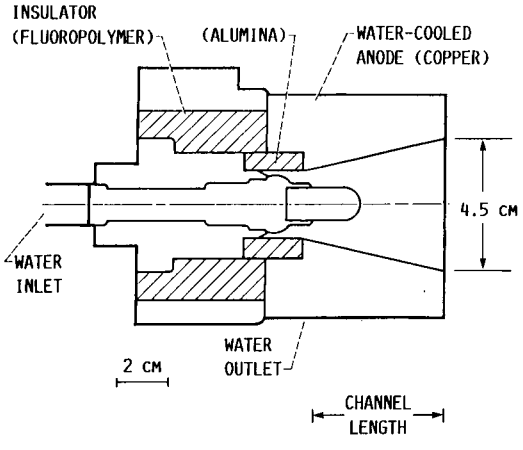

(C) MPD THRUSTER (E OR F) WITH CONICAL ANODE.

FIGURE 1. - SKETCHES OF MPD THRUSTERS.

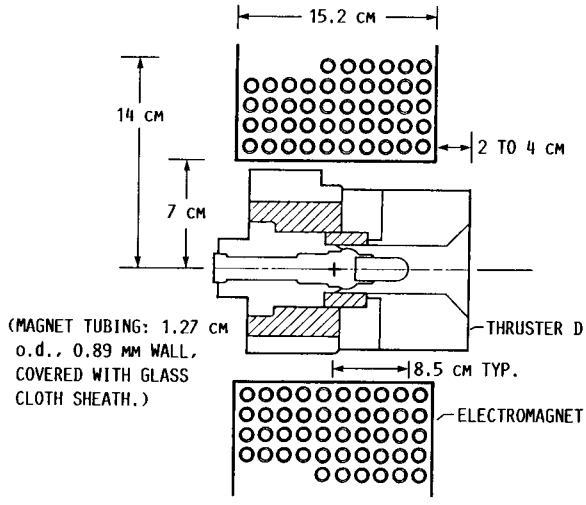

FIGURE 2. - SKETCH OF THRUSTER AND MAGNET ARRANGEMENT.

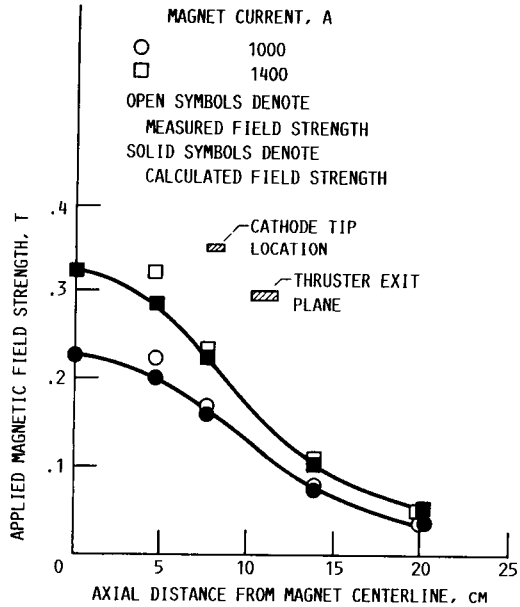

FIGURE 3. - COMPARISON OF CALCULATED AND MEASURED AXIAL MAGNETIC FIELD STRENGTH. (REF. 6).

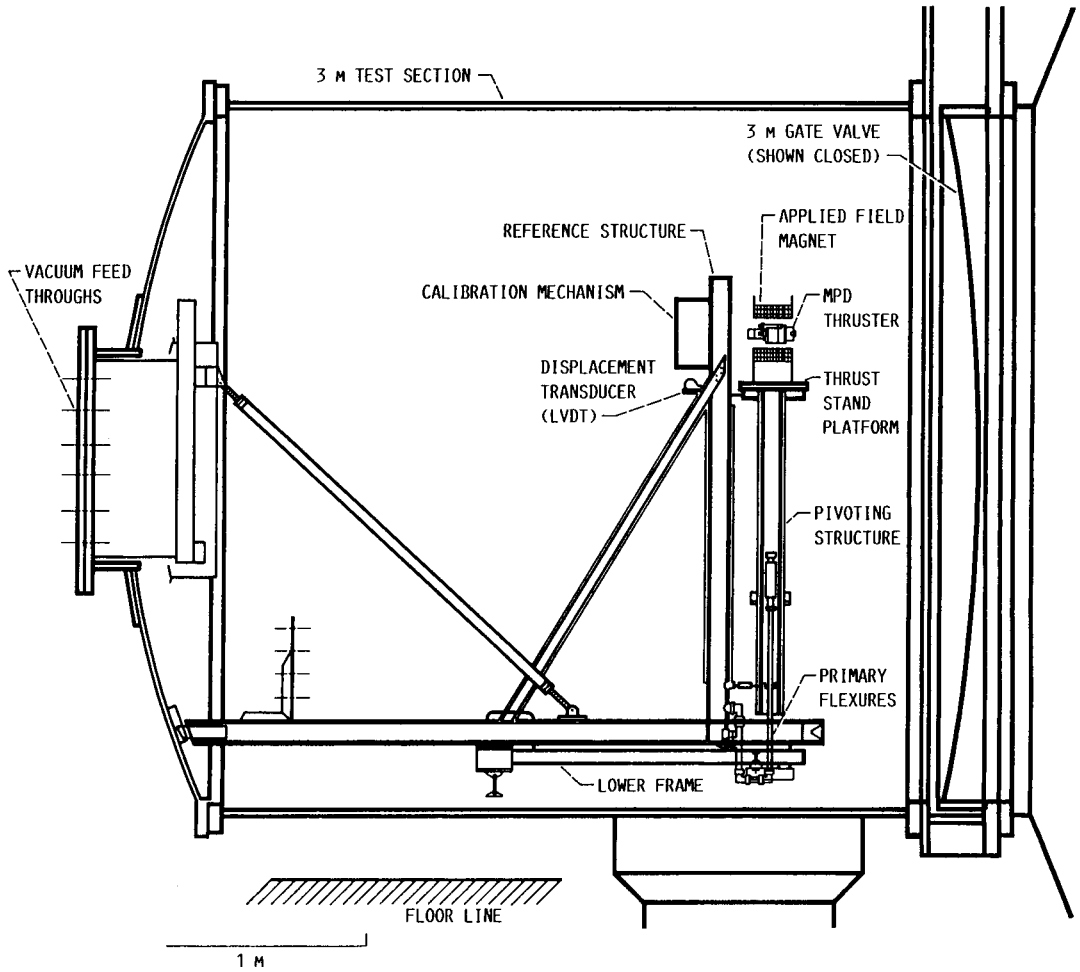

FIGURE 4. - SCHEMATIC OF MPD THRUSTER WITH THRUST STAND. (REF. 6).

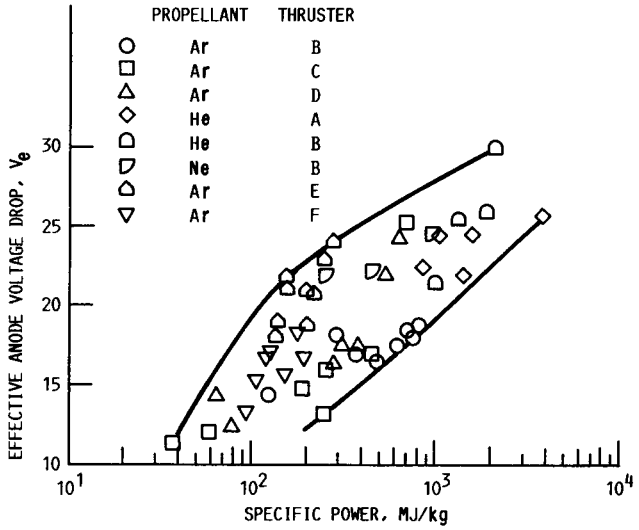

FIGURE 5. - EFFECTIVE ANODE VOLTAGE DROP VERSUS SPECIFIC POWER.

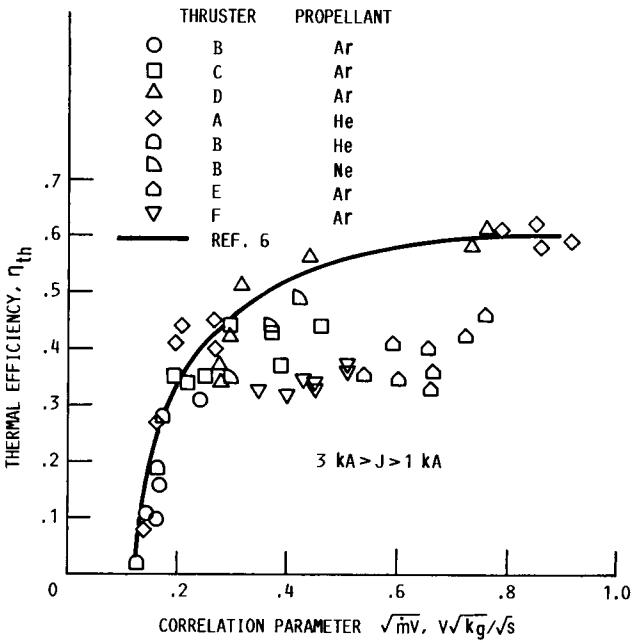

FIGURE 6. - THERMAL EFFICIENCY CORRELATION.

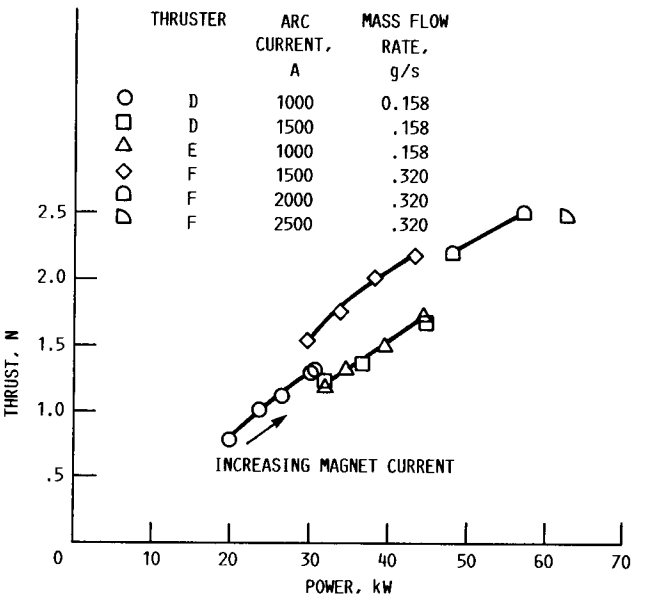

FIGURE 7. - THRUST AS A FUNCTION OF POWER.

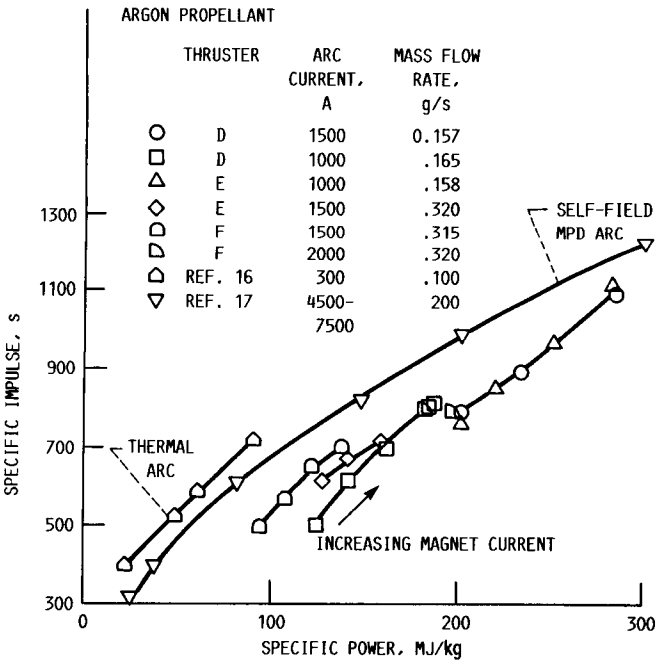

FIGURE 8. - SPECIFIC IMPULSE AS A FUNCTION OF SPECIFIC POWER.

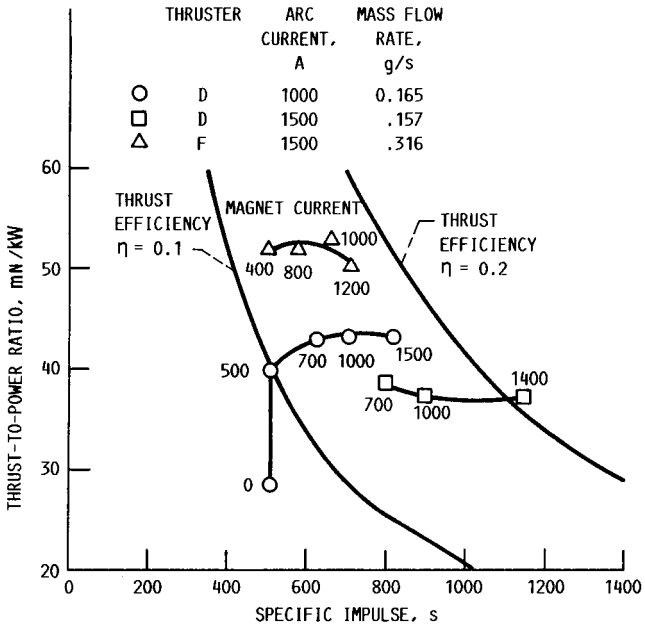

FIGURE 9. - THRUST-TO-POWER RATIO AS A FUNCTION OF SPECIFIC IMPULSE.

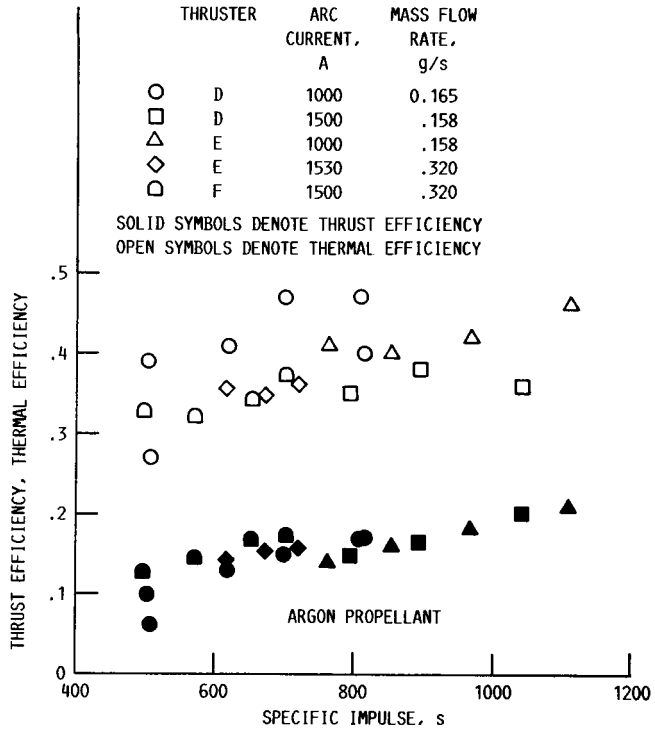

FIGURE 10. - THERMAL AND THRUST EFFICIENCY VERSUS SPECIFIC IMPULSE.

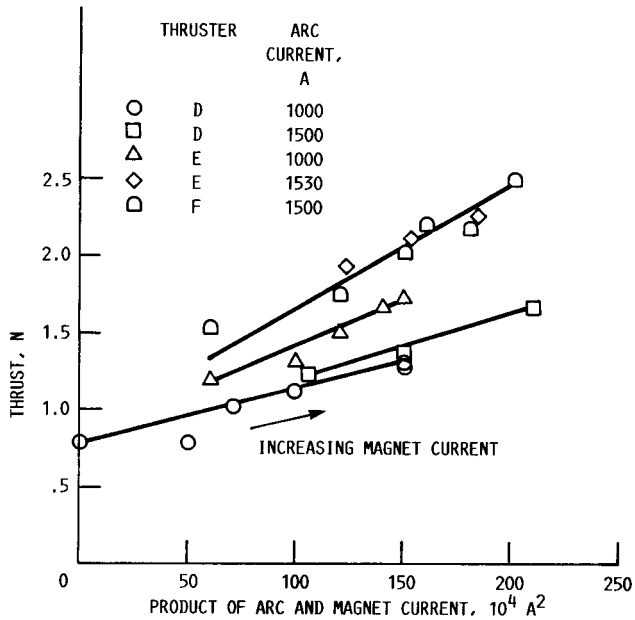

FIGURE 11. - THRUST AS A FUNCTION OF THE PRODUCT OF ARC CURRENT AND MAGNET CURRENT.

NASA
National Aeronautics and Space Administration

Report Documentation Page

1. Report No.	2. Government Accession No.	3. Recipient's Catalog No.
NASA TM-102312 AIAA-89-2710		

4. Title and Subtitle

Performance of a 100 kW Class Applied Field MPD Thruster

5. Report Date

6. Performing Organization Code

7. Author(s)

Maris A. Mantenieks, James S. Sovey, Roger M. Myers,
Thomas W. Haag, Paul Raitano, and James E. Parkes

8. Performing Organization Report No.

E-5006

10. Work Unit No.

506-42-31

9. Performing Organization Name and Address

National Aeronautics and Space Administration
Lewis Research Center
Cleveland, Ohio 44135-3191

11. Contract or Grant No.

13. Type of Report and Period Covered

Technical Memorandum

12. Sponsoring Agency Name and Address

National Aeronautics and Space Administration
Washington, D.C. 20546-0001

14. Sponsoring Agency Code

15. Supplementary Notes

Prepared for the 25th Joint Propulsion Conference cosponsored by the AIAA, ASME, SAE, and ASEE, Monterey, California, July 10-12, 1989. Maris A. Mantenieks, James S. Sovey, Thomas W. Haag, and Paul Raitano, NASA Lewis Research Center; Roger M. Myers and James E. Parkes, Sverdrup Technology, Inc., NASA Lewis Research Center Group, Cleveland, Ohio 44135.

16. Abstract

Performance of a 100 kW, applied field MPD thruster was evaluated and sensitivities of discharge characteristics to arc current, mass flow rate, and applied magnetic field were investigated. Thermal efficiencies as high as 60% thrust efficiencies up to 21%, and specific impulses of up to 1150 s were attained with argon propellant. Thrust levels up to 2.5 N were directly measured with an inverted pendulum thrust stand at discharge input powers up to 57 kW. It was observed that thrust increased monotonically with the product of arc current and magnet current.

17. Key Words (Suggested by Author(s))	18. Distribution Statement
MPD thrusters Electric propulsion	Unclassified – Unlimited Subject Category 20

19. Security Classif. (of this report)	20. Security Classif. (of this page)	21. No of pages	22. Price*
Unclassified	Unclassified	18	A03

*For sale by the National Technical Information Service, Springfield, Virginia 22161